Purpose-built Multicomponent Supramolecular Silver(I)-Hydrogels as Membrane-targeting Broad-spectrum Antibacterial Agents Against Multidrug-resistant Pathogens

Ekata Saha,[a,b] Afruja Khan,[c] Amirul Islam Mallick,[c*] and Joyee Mitra[a,b*]

[a] Inorganic Materials & Catalysis (IMC) Division, CSIR-Central Salt & Marine Chemicals Research Institute, Gijubhai Badheka Marg, Bhavnagar-364002, Gujarat, India.

[b] Academy of Scientific and Innovative Research (AcSIR), Ghaziabad-201002, U.P. India.

[c] Department of Biological Sciences, Indian Institute of Science Education and Research Kolkata, Mohanpur, Nadia, West Bengal-741246, India

E-mail: joyeemitra@csmcri.res.in, joyeemitra@gmail.com
amallick@iiserkol.ac.in

No. of Pages: 26 (S1 – S26)
Figures: 16 (S1 – S16)
Tables: 5 (S1 – S5)

Index

Experimental details

All reagents and solvents were commercially available and used as received without further purification. Silver Nitrate ($AgNO_3$), hydrochloric acid (HCl), sodium hydroxide (pellets), ammonia solution, glacial acetic acid, ethylenediaminetetraacetic acid (EDTA), lithium fluoride (LiF), sodium chloride (NaCl), sodium bromide (NaBr), potassium iodide (KI), sodium nitrate ($NaNO_3$), sodium acetate (NaOAc), sodium sulphate (Na_2SO_4), triphenylphosphine (PPh_3), tetra butyl ammonium bromide (TBABr) and urea were procured from Qualigens, Fisher Scientific, LobaChemie, Fisher Scientific, Fisher Scientific, Merck, Sigma Aldrich, Fisher Scientific, Qualigens, Qualigens, Fisher scientific, SD Fine Chemicals, LobaChemie, LobaChemie, SD Fine Chemicals and Merck respectively. Silver(I) trifluoromethanesulfonate (AgOTf) and 3,5-diamino-1,2,4-traizole were obtained from Sigma Aldrich and used as received. Mueller Hinton broth (HiMedia, India), Luria-Bertani broth media (HiMedia), Dimethyl sulfoxide (DMSO; Invitrogen), 4′,6-diamidino-2-phenylindole (DAPI; Sigma-Aldrich), Propidium Iodide (PI; Invitrogen), 2′,7′- Dichlorodihydrofluorescein diacetate (H_2DCFDA; Invitrogen) were used as received.

The synthesized metallogels and corresponding xerogels were characterized using several techniques such as PXRD, FT-IR, FESEM, TEM, TGA, ICP-MS and dynamic rheological studies. The powder X-ray diffraction (PXRD) analysis was done using Philips X'pert MPD system (PANalytical diffractometer) with Cu $K\alpha_1$ radiation (λ = 0.154 nm). The diffraction pattern was measured in the 2θ range from 5-90° at an operating voltage of 40 kV, 30 mA current, with a scan speed of 3º min^{-1} and a step size of 0.013º in 2θ at RT with a scan step time 58.395 sec. Anode material was Cu and the value of $K_{\alpha1}$, $K_{\alpha2}$ and K_β were 1.54060 [Å], 1.54443 [Å] and 1.39225 [Å], respectively. Fourier transform Infrared Spectra analysis (FT-IR) was recorded on Perkin Elmer-Spectrum G-FTIR spectrometer (Germany) from 400-4000 cm^{-1} with a resolution of 4 cm^{-1} using KBr pellets. The surface morphology of the prepared gel material was analyzed by Field Emission-Scanning Electron Microscope (FESEM) (JEOL JSM 7100F) with an accelerating voltage of 5–15 kV with 10 μA of emission current. The transition electron microscope (TEM) analysis was done with JEOL, JEM 2100 TEM instrument. The rheological properties of samples were measured by the Anton Paar Rheometer. For the amplitude sweep experiment (Dynamic strain sweep, DSS) and step-strain experiment, the operating frequency was kept constant at 1 rad s^{-1}. The operating strain was kept constant at 0.1% over the entire frequency range for the dynamic frequency sweep measurements. The xerogels (lyophilized powder derived from the corresponding metallogels) were prepared by freeze-drying (lyophilizing) method using a VirTis freezemobile 25EL lyophilizer.

The absorbance of bacterial culture was measured using Epoch2 microplate reader (BioTek, USA). The bacterial morphology (FE-SEM images) was examined using a Carl Zeiss SUPRA 55 V P FE-SEM (Germany). The total vs. dead cell population in the bacterial cells was imaged using a confocal laser scanning microscope (Leica Microscope, Wetzlar, Germany) with the HC PL APO CS2

63×/1.4 oil immersion lens, 405 nm laser for DAPI stained bacteria and 488 nm laser for PI. The intracellular ROS generation was measured by taking the fluorescence intensity of each sample using Spectramax M2e Multi Detection Microplate Readers (Molecular Devices LLC, USA) with the excitation and emission wavelengths at 485 nm and 535 nm, respectively.

Cell Cytotoxicity of AgDU-Xerogels:

To determine the cytotoxic effect of **AgDU-Xerogels** against human Caco-2, HEK293T and INT407 the 50% cytotoxic concentration (CC_{50}) was determined by standard 3-(4,5-dimethylthiazol-2-yl)-2,5-diphenyl tetrazolium bromide (MTT) assay.[1] In brief, each type of cell (1.5×10^4 cells/well) was seeded in a 96 well plate and maintained in growth medium (containing Dulbecco's modified eagle medium (DMEM; Gibco, Invitrogen, Thermo Scientific, USA) supplemented with 10 % fetal bovine serum (Gibco, Invitrogen, Thermo Scientific), 100 U/mL penicillin and 100 µg/mL streptomycin). At 80% confluence, cells were treated with different concentrations of **AgDU-Xero1** and **AgDU-Xero2** (ranging from 1.95-250 µg/mL) and incubated for 24 h at 37 °C under 5% CO2 pressure. After the incubation, cells were washed with PBS and again incubated with fresh growth media containing MTT dye (final concentration 100 µg/mL) for another 3 h. Next, formazan crystals were dissolved in DMSO, and the absorbance was measured at 595 nm using a microplate reader (Epoch2, BioTek, USA). Cell viability was calculated according to the following equation:

Cell viability (%) $=(A_{Tr}/A_C) \times 100$

where, A_{Tr} is the absorbance of cells treated with **AgDU-Xerogels** and A_C is the absorbance of untreated cells. CC_{50} value was calculated from dose-response curves of the cell viability versus concentration graphs, plotted using GraphPad Prism 8.

Exploration of Antibacterial activity of AgDU-Xerogels

Assessing the Minimum Inhibitory Concentrations (MIC) of AgDU-Xero1 and AgDU-Xero2 against *C. jejuni* and *S. aureus*:

The assessment of MIC of **AgDU-Xero1** and **AgDU-Xero2** against the test bacteria was performed using the micro broth dilution method as described earlier with some modification.[2] In brief, both bacteria were separately grown for 24 h in respective growth media. Next, the bacterial culture was diluted to an optical density of 0.4 at 600 nm (OD_{600}) in the growth medium and 50 µL of bacterial culture was added to each well of a 96-well plate. After that, different concentrations of **AgDU-Xero1** and **AgDU-Xero2** were prepared in 0.1% DMSO (v/v), ranging from 0 to 250 µg/mL. Finally, 50 µL from each dilution was added to the plates and incubated for 24 h. Next day, the absorbance was

measured (OD_{600}) in a microplate reader (Epoch2, BioTek, USA). The MIC was calculated from the absorbance values that depicted a 50% retardation in bacterial growth as per the following formula:

$$\text{Bacterial viability} = [(OD_{compound}/OD_{control}) \times 100]$$

Where $OD_{compound}$ is the absorbance value of bacterial suspension treated with each concentration of test compound, $OD_{control}$ is the absorbance value of bacterial suspension without any treatment.

The MIC_{50} of hydrogels value was at which 50 % retardation in bacterial growth was visible.

Antibacterial effect of AgDU-Xero1 and AgDU-Xero2

Comparative analysis of the anti-bacterial effect of multi-component xerogel vs single component: Antibacterial activity of multicomponent xerogels, such as **AgDU-Xero1** and **AgDU-Xero2** were evaluated against both the bacteria by counting the colony-forming units (CFU) at 5 h post-treatment time point.[3] Briefly, the bacterial strains were grown separately in MH and LB media. Three different concentrations (40 μg/mL, 60 μg/mL, and 80 μg/mL) of **AgDU-Xero1** and **AgDU-Xero2** were chosen. Each concentration of the test compounds was then co-incubated with the test bacteria for 5 h. After the incubation, the suspensions were plated onto MH or LB agar plates, respectively. Untreated and DMSO (0.1 %; vehicle control) treated bacterial cultures served as controls. Finally, after 24-48 h of incubation, the resulting bacterial colonies on the plate were counted. All the experiments were carried out in triplicate and calculated as mean CFU/mL ± SE.

To assess the antibacterial activity of the individual components (such as AgOTf, $AgNO_3$, Urea and DATr) of **AgDU-Xero1**, and **AgDU-Xero2**, the same experimental set-up was used. For comparative analysis (multicomponent vs individual components), we choose to use MIC_{50} of **AgDU-Xero1** and **AgDU-Xero2** as standard for determining the antibacterial efficacy of individual components **(**DATr, Urea, and $AgNO_3$/AgOTf**)**. The bacterial cells were incubated with the following concentration of multicomponent xerogels and their respective compositional components as mentioned below:

AgDU-Xero1 (60 μg/mL) contains [**Ag(I)** (15.02 μg/mL)[#] + **Urea** (8.64 μg/mL)+ **DATr** (14.4 μg/mL)]* (**Figure S16a**);
AgDU-Xero2 (60 μg/mL) contains [**Ag(I)** (16.56 μg/mL)[#] + **Urea** (10.86 μg/mL) + **DATr** (18.18 μg/mL)]* (**Figure S16b**)
*The final concentration of individual components is used to test antibacterial efficacy.

[#]Concentration of **Ag(I)** calculated from ICP-MS analysis **(Table S1)**.

Bacterial cell viability: To assess the viability of bacterial cells treated with **AgDU-Xero1** and **AgDU-Xero2**, the ratio of total vs. dead bacteria was calculated at 5 h post-treatment. To differentiate live and dead cells, we performed a dual staining method with DAPI as a cell-permeable dye (to stain both dead and live bacteria) and propidium iodide as a cell-impermeable dye (to stain the dead bacterial population only).[4] For this, bacterial cells incubated (5 h) with different concentrations (40 μg/mL, 60 μg/mL, and 80 μg/mL) of **AgDU-Xero1** and **AgDU-Xero2**, were centrifuged, washed, resuspended in PBS, followed by adding 1 μL of PI (1 mg/mL) and 1 μL of DAPI (1 mg/mL). The samples were gently tapped and incubated for 30 min at room temperature (RT). Then the samples were washed 2-3 times to remove excess dye molecules. Finally, the samples were loaded on a glass slide by drop casting method and observed under a confocal laser scanning microscope (Leica) using 405 nm laser for DAPI and 488 nm laser for PI.

Induction of oxidative stress in bacteria: Given that Reactive Oxygen Species (ROS) are constantly generated as secondary metabolites of some biological processes, we assessed the gel's ability to facilitate oxidative damage on the test bacteria as per the method described previously.[5] Briefly, bacterial suspension was incubated with **AgDU-Xero1** and **AgDU-Xero2** (final concentration 60 µg/mL) for 30 min, 1 h, and 2 h. Next, 200 µL of H_2DCFDA (20 µM) in 1X PBS was added and incubated for 1 h. Finally, intracellular ROS generation was measured by taking the fluorescence intensity of each sample using Spectramax M2e Multi Detection Microplate Readers (Molecular Devices LLC, USA) with the excitation and emission wavelengths at 485 nm and 535 nm, respectively.

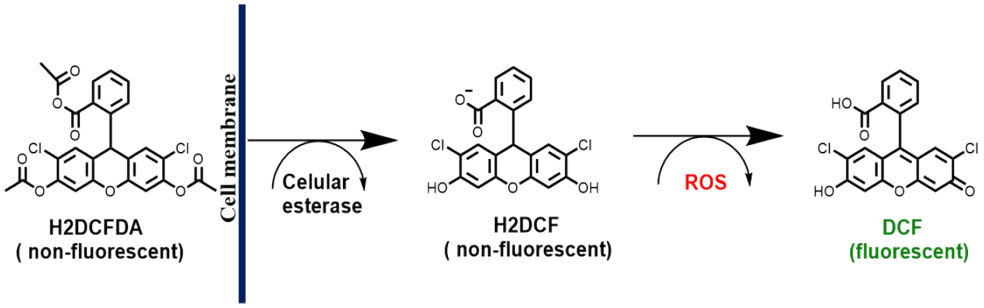

Effect of AgDU-Xero1 and AgDU-Xero2 on bacterial morphology.

The morphological changes of *S. aureus* and *C. jejuni* after treatment with the test compounds were examined by FE-SEM images (Carl Zeiss SUPRA 55 V P FE-SEM) as per the method described previously.[6] Briefly, *S. aureus* and *C. jejuni* co-incubated with different concentrations (40 and 60 µg/mL) of **AgDU-Xero1** and **AgDU-Xero2** for 5 h, respectively. Post-incubation, cells were washed with sterile 1X PBS and fixed for 2 h in 2.5% (v/v) glutaraldehyde (prepared in PBS; pH 7.4) at RT. Fixed samples were washed thrice with PBS, followed by sequential dehydration in 35%, 50%, 70%, and 95% ethanol for 10 min each and 100% ethanol for 1 h for complete dehydration. The fixed and dehydrated samples were drop-casted on the coverslip and vacuum-dried overnight. The samples were thoroughly dried under vacuum, fixed to aluminium stubs with silver conductive paint, sputter-coated with gold, and examined using a Supra 55 Carl Zeiss scanning electron microscope.

Data analysis

The OriginPro 8.5 and GraphPad Prism statistical software (version 8) were used for graphical presentations and data analysis.

Analytical Data

Mass analysis for the gels

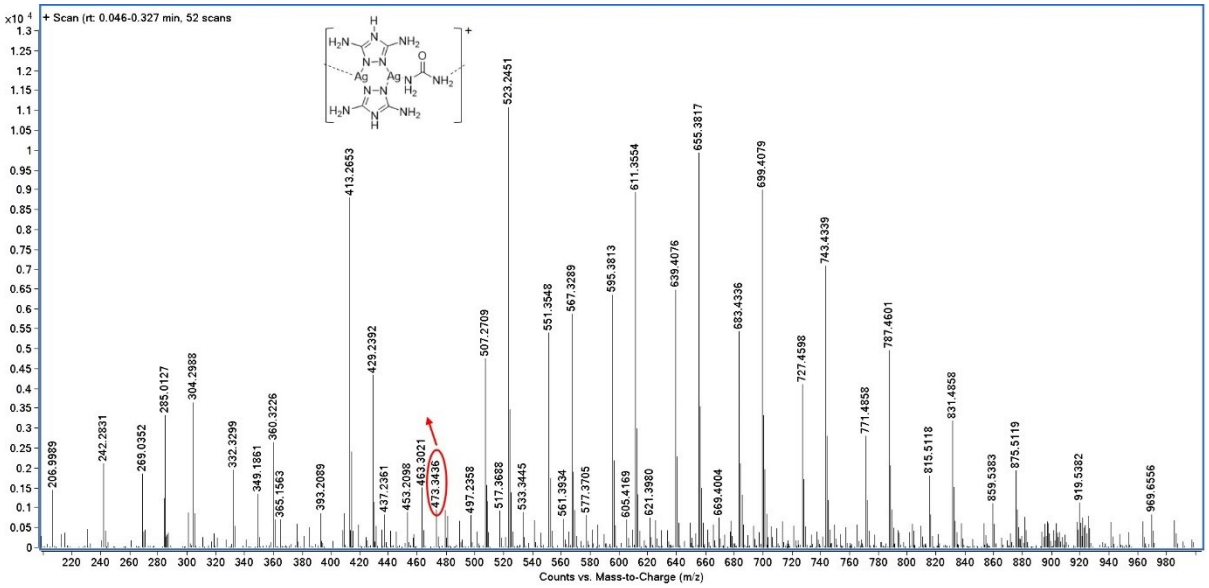

Figure S1. Mass spectral pattern of **AgDU-Gel1** showing the repeating unit of the gel as $C_5H_{14}Ag_2N_{12}O$ (theoretical m/z = 473.95, observed m/z = 473.34).

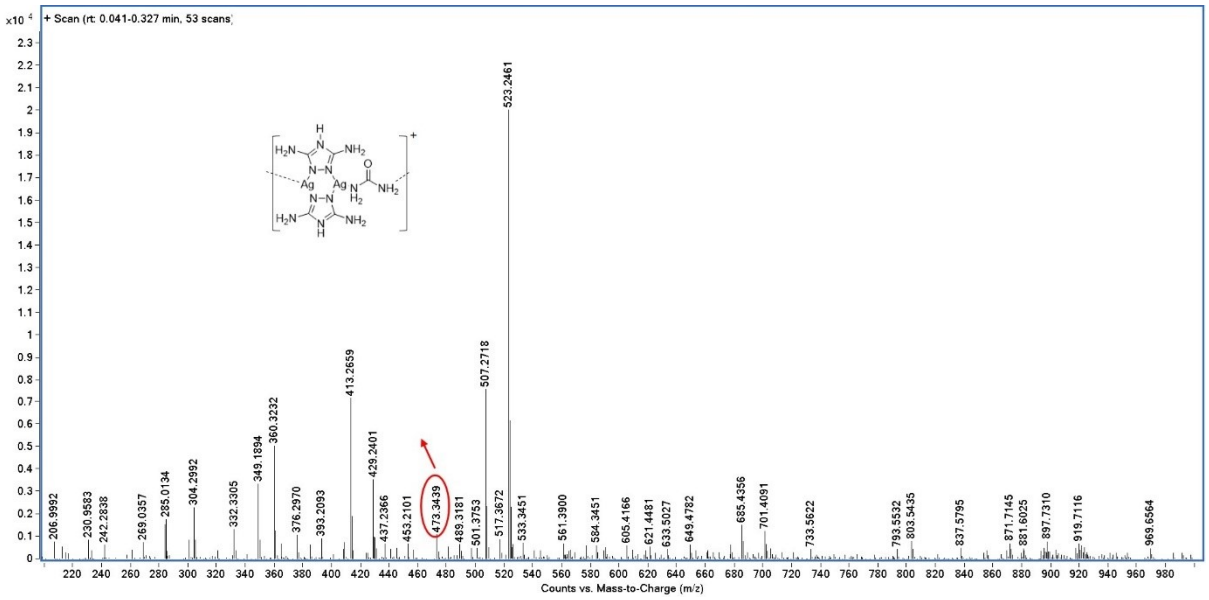

Figure S2. Mass spectral pattern of **AgDU-Gel2** showing the repeating unit of the gel as $C_5H_{14}Ag_2N_{12}O$ (theoretical m/z = 473.95, observed m/z = 473.34).

Evaluation of the minimum gelator concentration (MGC) for the gels

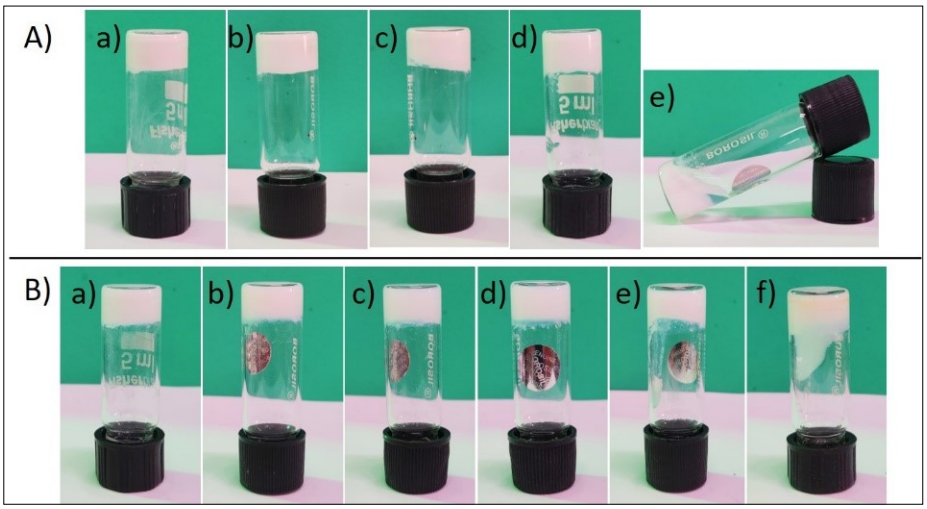

Figure S3. Evaluation of minimum gelator concentration (MGC) for the gels Panel-A) **AgDU-Gel1**, and Panel-B) **AgDU-Gel2** respectively. In all the cases from A) and B), the evaluation performed for a) 0.5 mmol, b) 0.25 mmol, c) 0.2 mmol, d) 0.15 mmol, e) 0.125 and f) 0.1 mmol for each of Ag(I) precursor, DATr and urea concentration.

FT-IR spectra of the gels and xerogels

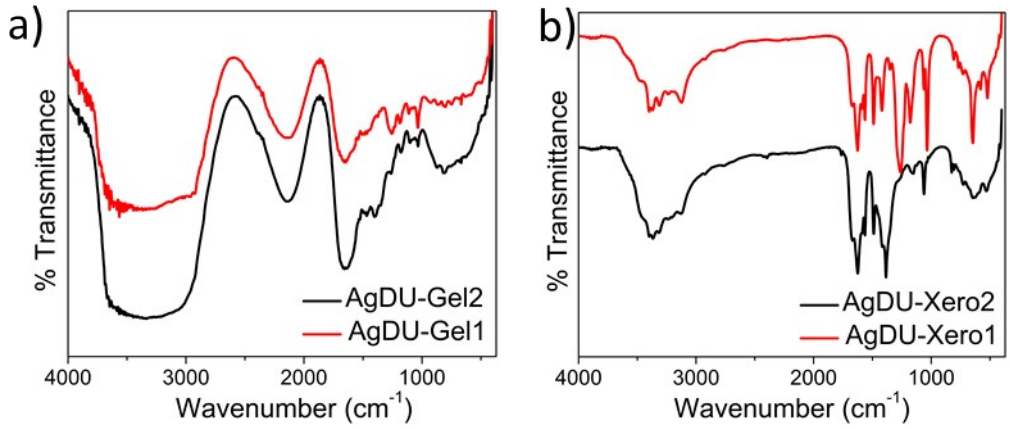

Figure S4. FT-IR spectra of the gels (and corresponding xerogels). a) **AgDU-Gel1** and **AgDU-Gel2**; b) **AgDU-Xero1** and **AgDU-Xero2,** respectively.

FE-SEM images of gel-derived xerogels

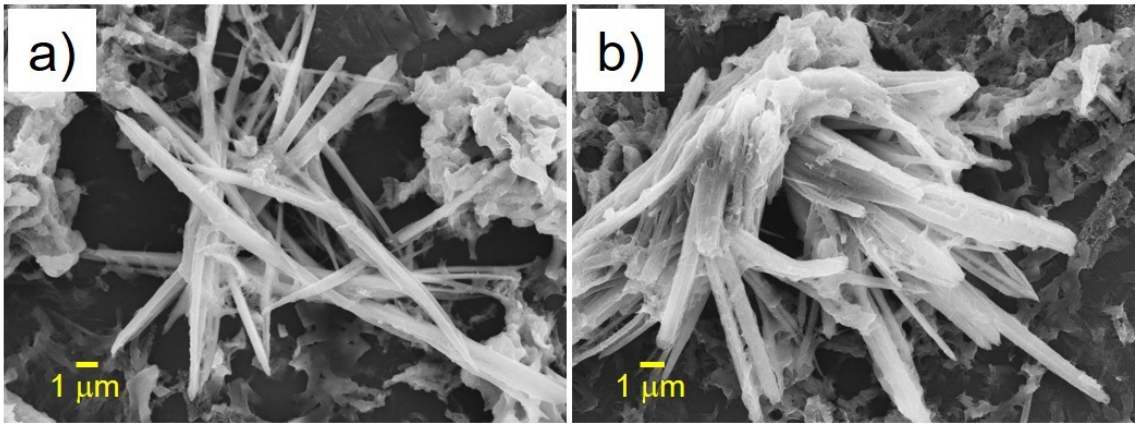

Figure S5. (a) and (b) FE-SEM images of the gel-derived xerogel **AgDU-Xero1** showing fibrous morphology.

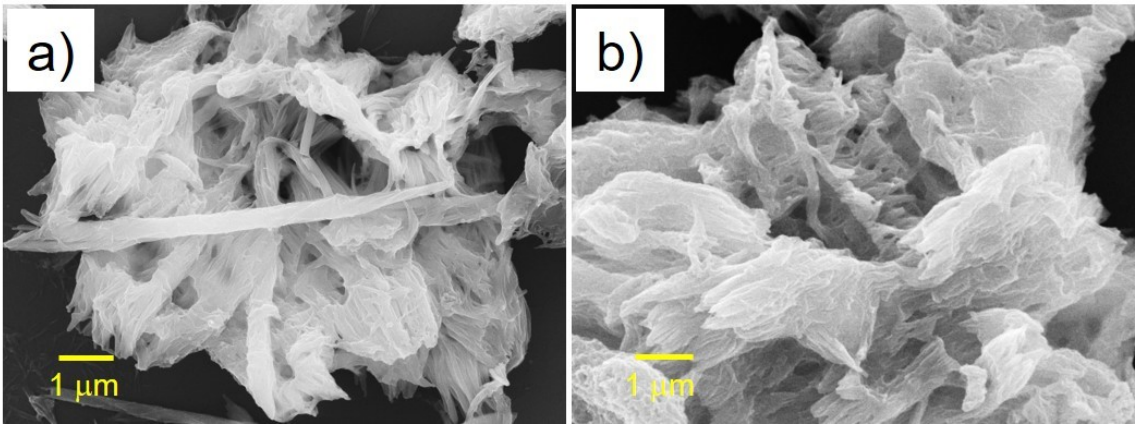

Figure S6. (a) and (b) FE-SEM images of the gel-derived xerogel **AgDU-Xero2** showing fibrous morphology.

TEM images of gel-derived xerogels

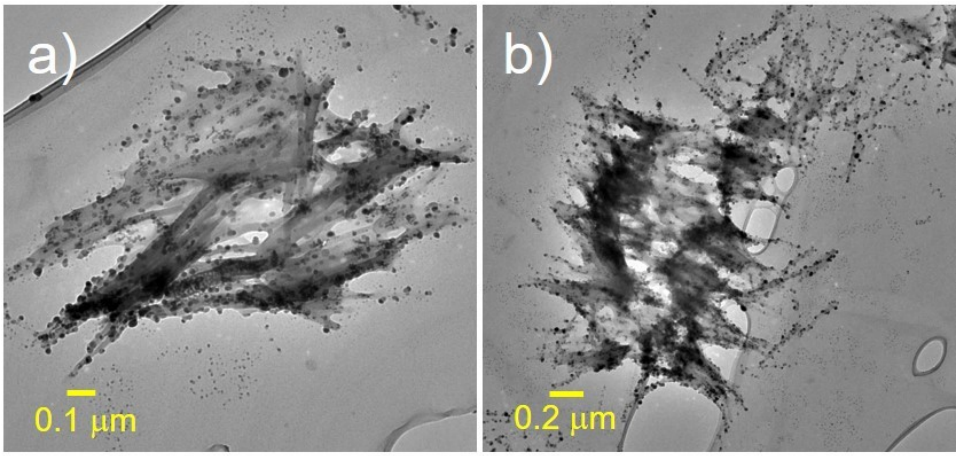

Figure S7. (a) and (b) TEM images of the gel-derived xerogel **AgDU-Xero1** showing fibrous morphology.

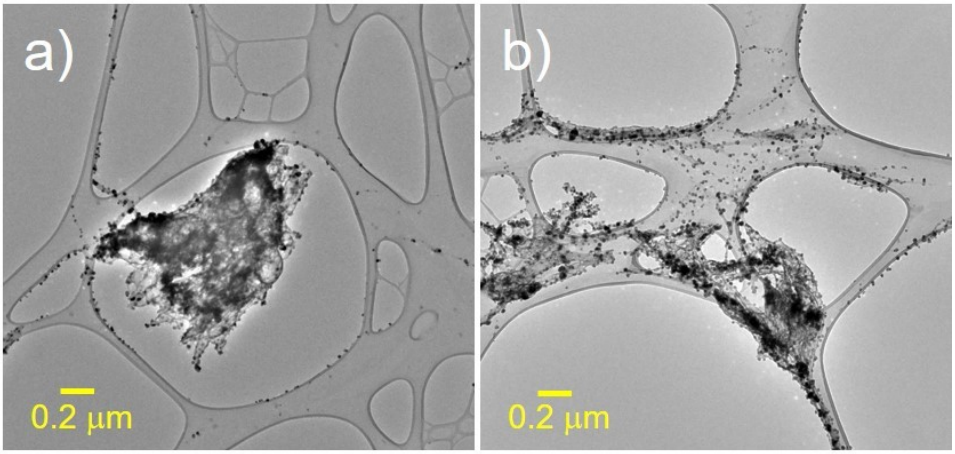

Figure S8. (a) and (b) TEM images of the gel-derived xerogel **AgDU-Xero2** showing fibrous morphology.

XPS spectra of the gel-derived xerogels

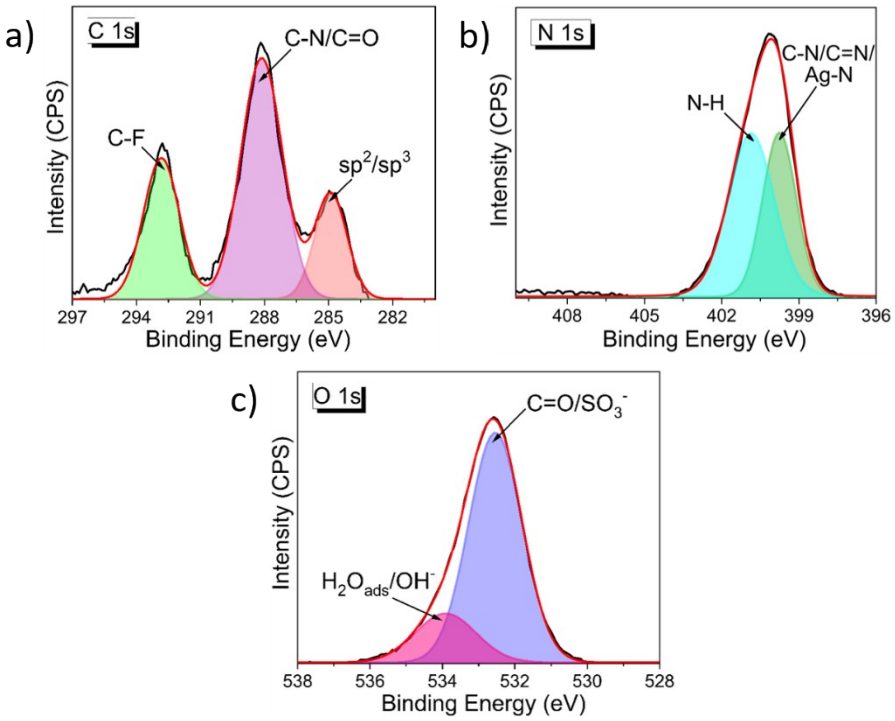

Figure S9. High-resolution XPS data depicting the presence of a) C, b) N and c) O, respectively, in the gel-derived xerogel **AgDU-Xero1**.

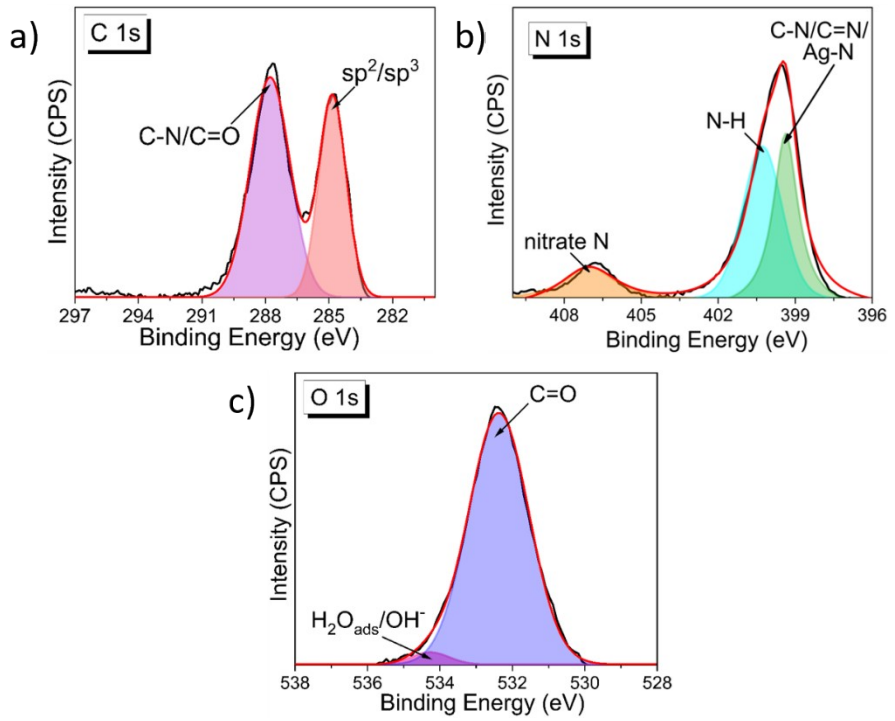

Figure S10. High-resolution XPS data depicting the presence of a) C, b) N and c) O, respectively, in the gel-derived xerogel **AgDU-Xero2**.

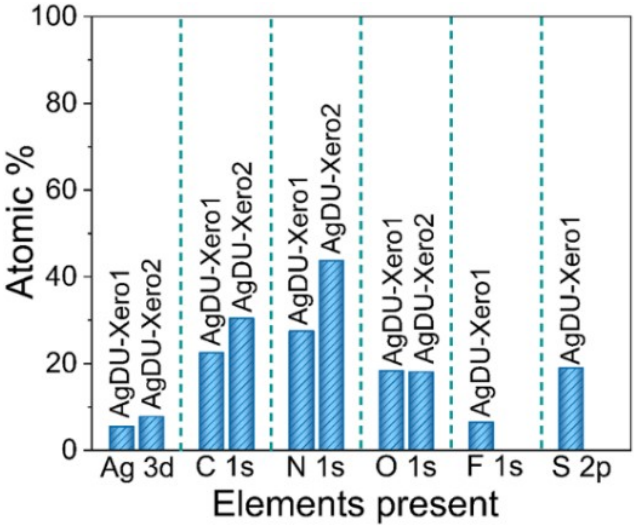

Figure S11. Surface atomic percentage of the constituent elements in the gel-derived xerogels **AgDU-Xero1** and **AgDU-Xero2**.

TGA measurements of the gel-derived xerogels

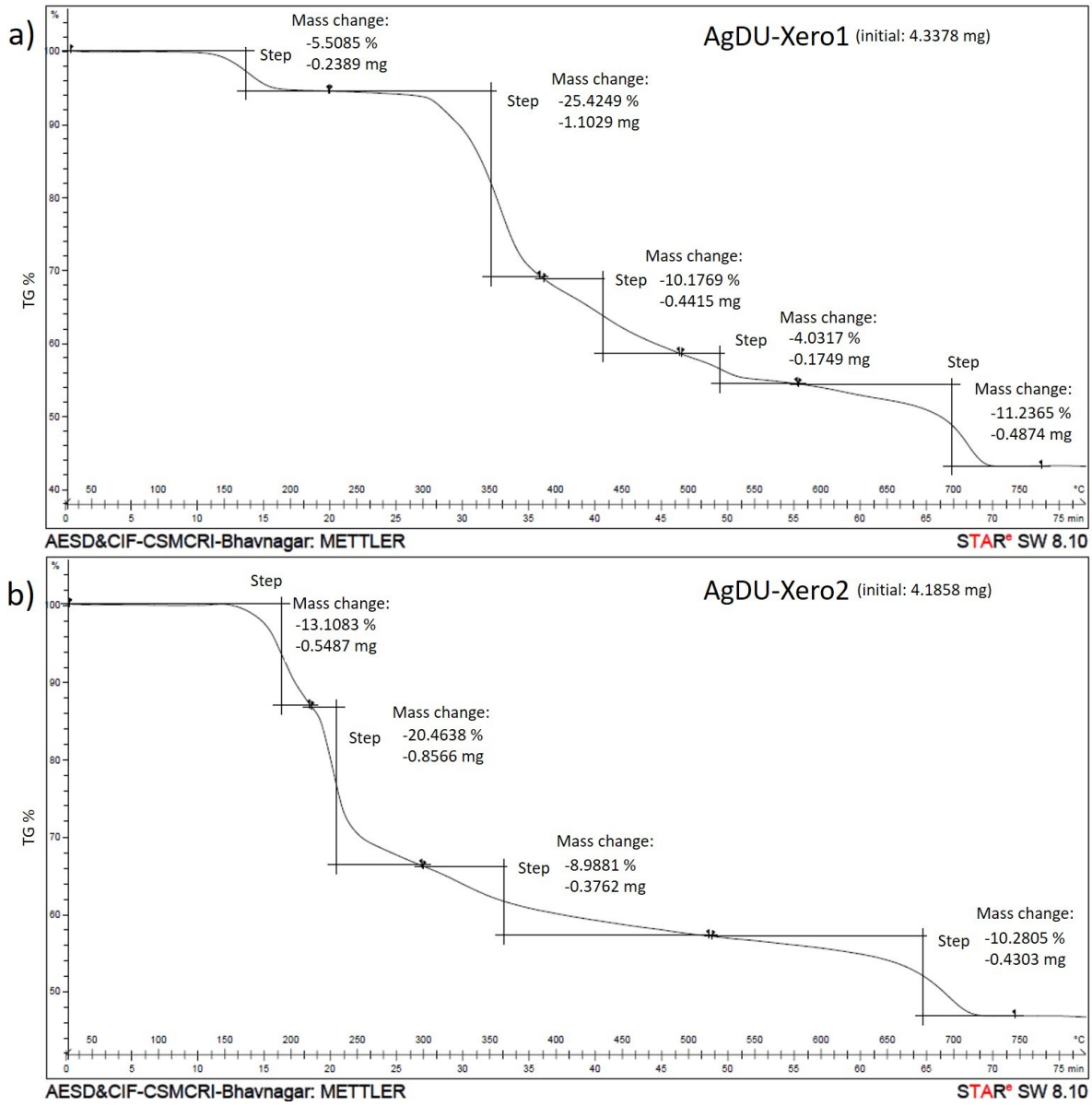

Figure S12. TGA analysis of the gel-derived xerogel a) **AgDU-Xero1** and b) **AgDU-Xero2**.

Stimuli-responsive nature of Ag(I)-hydrogels

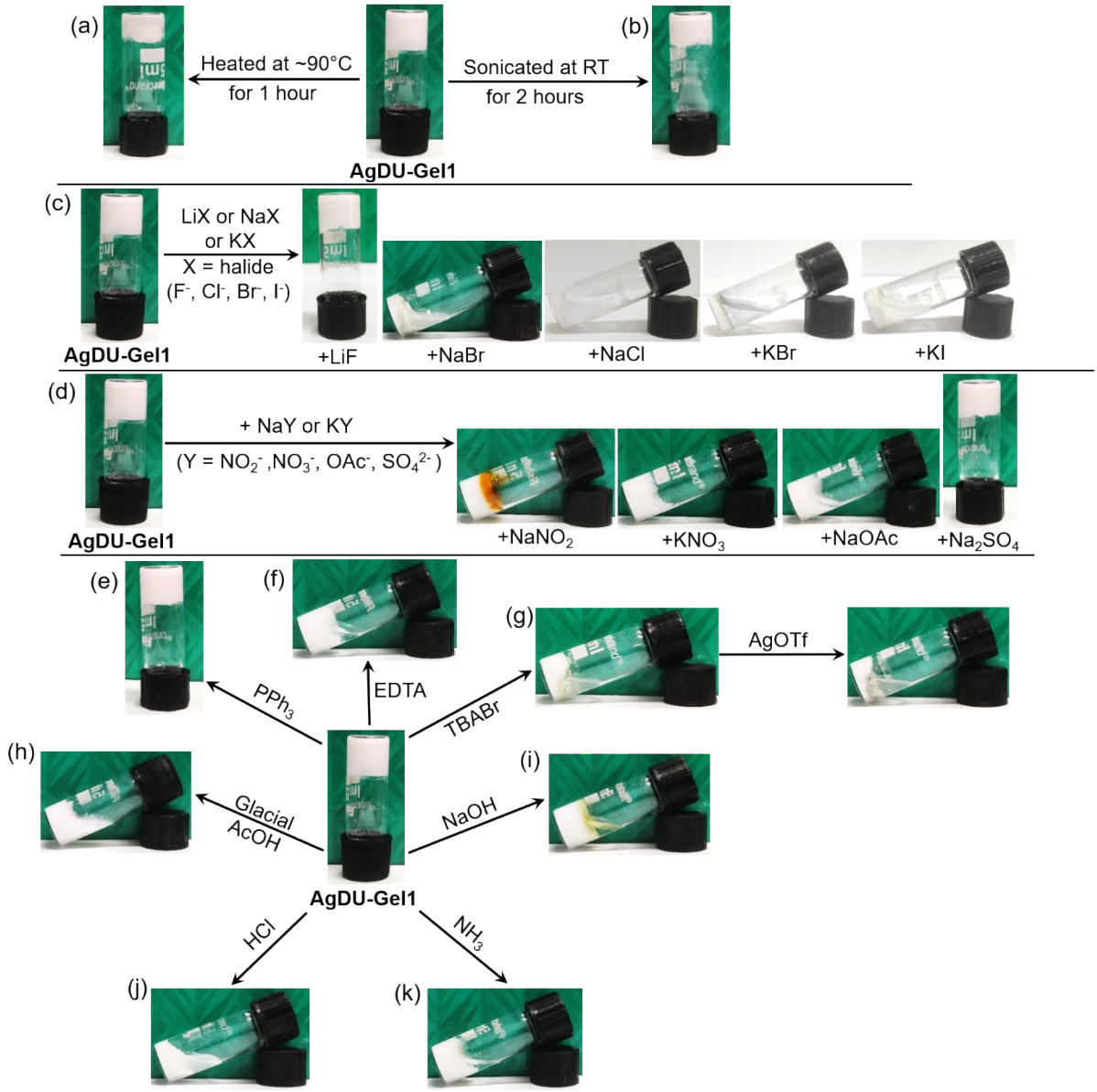

Figure S13. Detailed depiction of the stimuli-responsive nature of **AgDU-Gel1**.

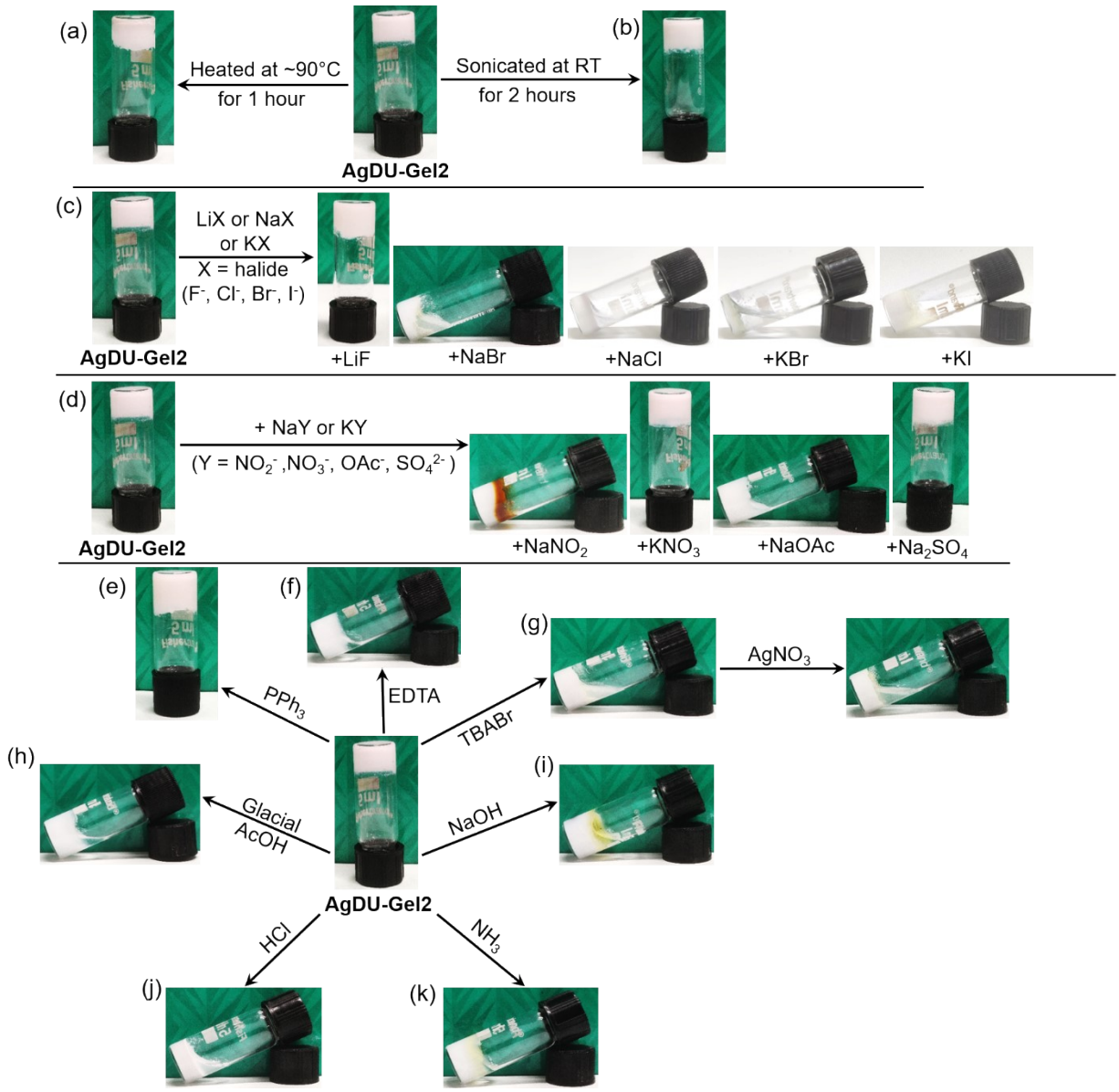

Figure S14. Detailed depiction of the stimuli-responsive nature of **AgDU-Gel2**.

Cytotoxic effect of AgDU-xerogels

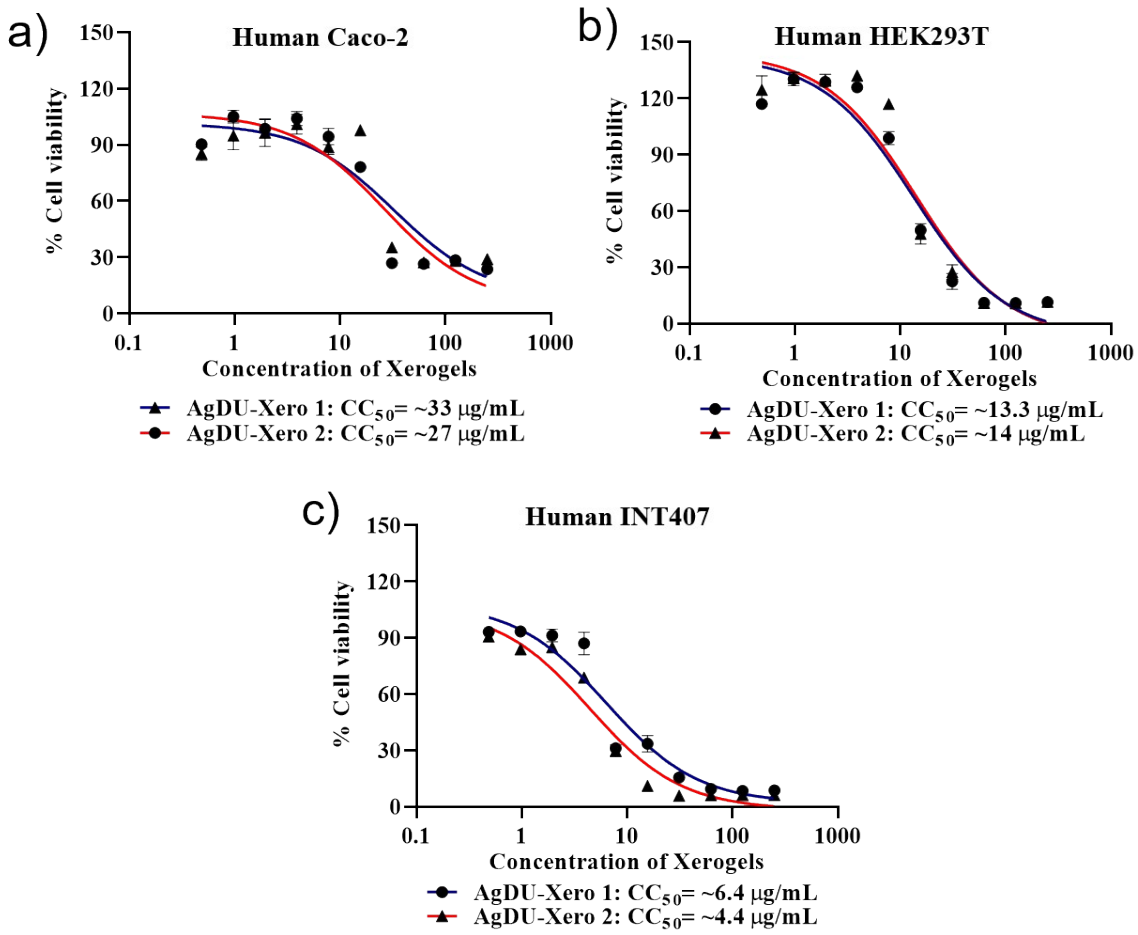

Figure S15. Cytotoxic effect of AgDU-Xerogels. The CC_{50} of xerogels was calculated by standard MTT assay. Human Caco-2 (a), Human HEK293T (b) and Human INT407 (c) cells were treated with different concentrations of AgDU-Xerogels (ranging from 0 µg/mL to 250 µg/mL) and incubated for 24 h. The data suggest that the CC_{50} value of **AgDU-Xero1** is ~33 µg/mL for Caco-2, ~13.3 µg/mL for HEK293T and ~6.4 µg/mL for INT407 cells. The CC_{50} value of **AgDU-Xero2** is ~27 µg/mL for Caco-2, ~14 µg/mL for HEK293T and ~4.4 µg/mL for INT407 cells. Individual dots represent the Mean percentage of cell viability ± SE.

Antibacterial effect of multi-component xerogels vs single components

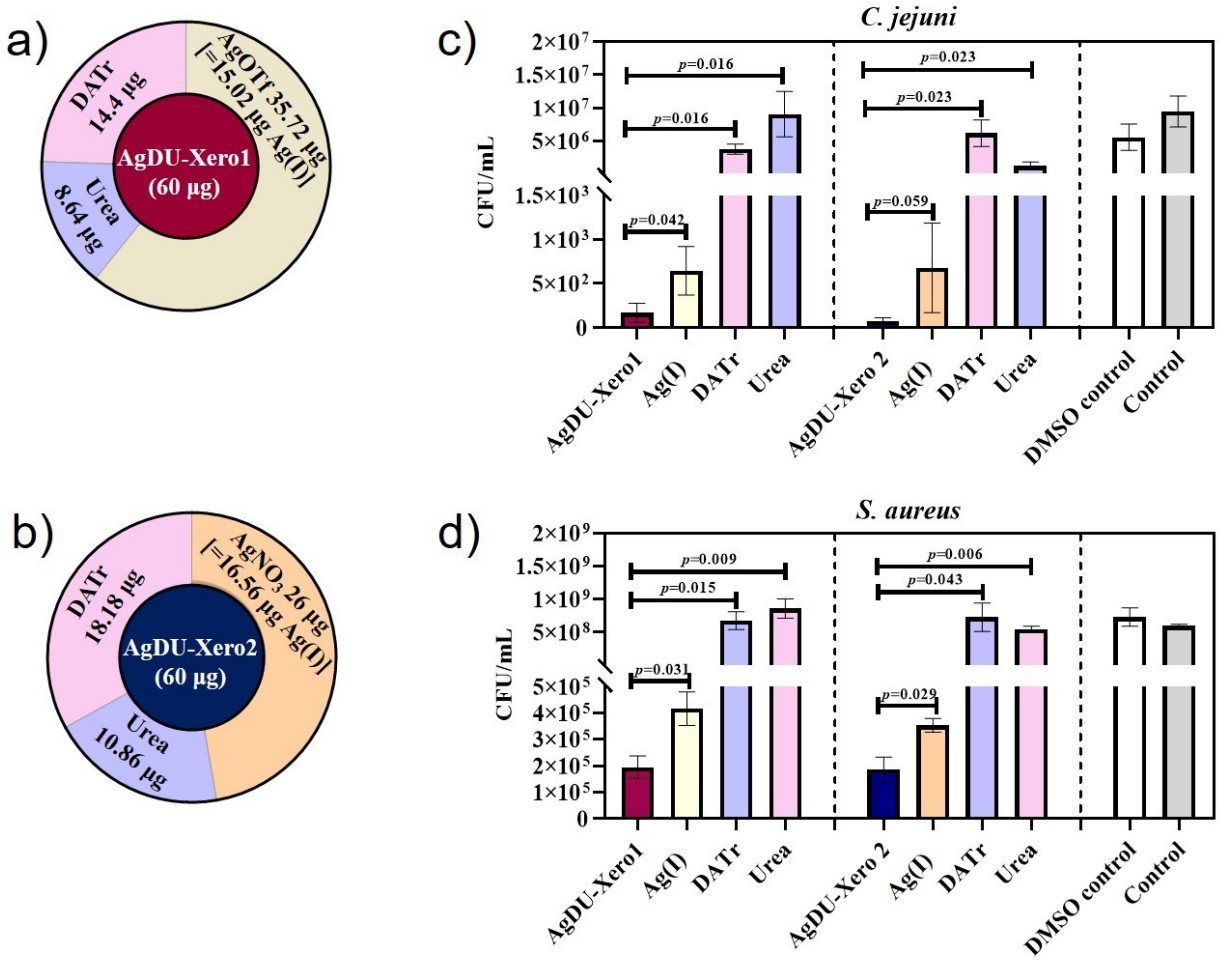

Figure S16. Antibacterial effect of multi-component xerogels vs single components. Representative of Gram-positive bacteria (*S. aureus*) and Gram-negative bacteria (*C. jejuni*) were incubated with **AgDU-Xero1** (60 µg/mL) contains Ag(I) (15.02 µg/mL) + Urea (8.64 µg/mL) + DATr (14.4 µg/mL) (a); **AgDU-Xero2** (60 µg/mL) contains Ag(I) (16.56 µg/mL) + Urea (10.86 µg/mL) + DATr (18.18 µg/mL) (b) at 37 ℃ for 5 h. Next, approximately 50 µL culture from each set was plated on respective agar plates, and the resulting colonies were counted. For the bacteria, either *C. jejuni* (c) or *S. aureus* (d), treatment with multi-component xerogels (**AgDU-Xero1** and **AgDU-Xero2**) showed a significant reduction of bacterial count compared to the single components. The data are presented as mean CFU/mL ± SE from three independent experiments. $p \leq 0.05$ were considered statistically significant.

Table S1. ICP-MS Analysis of the gels and corresponding xerogels

Sl. No.	Name of the compounds	Presence of Ag(I) content in 10 mg of samples
1.	AgDU-Gel1	0.668 mg
2.	AgDU-Gel2	0.796 mg
3.	AgDU-Xero1	2.504 mg
4.	AgDU-Xero2	2.761 mg

Table S2. Zeta potential measurements of the Ag(I)-hydrogels

Sl. No.	Name of the compounds	Zeta potential (ζ) values
1.	AgDU-Xero1 (triflate counter anion)	+18.1 mV
2.	AgDU-Xero2 (nitrate counter anion)	+17.4 mV

Table S3. Minimum Inhibitory Concentration (MIC) of AgDU-Xero1 and AgDU-Xero2

Compounds	Minimum Inhibitory Concentration (MIC_{50}) (µg/mL)	
	Gram-positive bacteria	Gram-negative bacteria
	S. aureus	*C. jejuni*
AgDU-Xero1	≥ 62.5	≥ 60
AgDU-Xero2	≥62.5	≥ 60

Table S4. Comparison table for antibacterial activities against Gram-negative *C. jejuni*

Sl. No.	Antibacterial Compound	Bacteria	MIC	References
1.	Silver(I)-hydrogel	*C. jejuni*	60 µg/mL	This work
2.	Medicinal plant Adenanthera pavonina	*C. jejuni*	62.5-125 µg/mL	7
3.	Flavonoids galangin and quercetin	*C. jejuni*	0.250-0.125 mg/mL	8
4.	Ciprofloxacin	*C. jejuni*	16 mg/L	9
5.	Erythromycin	*C. jejuni*	4-8 mg/L	9
6.	Cinnamon oil, (E)-cinnamaldehyde, clove oil, eugenol, and baicalein	*C. jejuni*	25–100 µg/mL	10
7.	polysaccharides (phenolic acid, flavonoid and other phenolic antimicrobials)	*C. jejuni*	256-1024 µg/mL	11
8.	Essential oil ((*E*)-Methylisoeugenol and Elemicin)	*C. jejuni*	250 µg/mL	12
9.	Phenolic compounds	*C. jejuni*	78-313 µg/mL	13
10.	allyl-isothiocyanate	*C. jejuni*	50–200 µg/mL	14
11.	Nanocarriers from natural lipids	*C. jejuni*	0.78-3 mg/mL	15
12.	Magnesium oxide nanoparticles	*C. jejuni*	0.5 mg/mL	16

Table S5. Comparison table for antibacterial activities against Gram-positive *S. aureus and MRSA*

Sl. No.	Antibacterial Compound	Bacteria	MIC	References
1.	Silver(I)-hydrogel	*S. aureus*	62.5 µg/mL	This work
2.	Medicinal plant Annona squamosa	*S. aureus*	62.5-125 µg/mL	7
3.	Curcumin	*S. aureus*	125-250 µg/mL	17
4.	oxacillin, and cefdinir (antibiotic)	*S. aureus*	≤ 0.06 mg/L	18
5.	Naringenin	*S. aureus*	200-400 µg/mL	19
6.	cysteine-rich cationic proteins	*S. aureus*	1-8 mg/L	20
7.	Silver nanoparticles	*S. aureus*	100 µg/mL	21
8.	Linezolid and Fosfomycin (antibiotic)	*S. aureus*	≥8 mg/L and >32 mg/L respectively	22
9.	tannic acid	*S. aureus*	40 to 160 µg/mL	23
10.	Silver nanoparticles	*S. aureus* and MRSA	62.5 and 125 µg/mL respectively	24
11.	AgNps and ZnNPs	*S. aureus* and MRSA	1.25-5 and 2.5 mg/mL respectively	25
12.	ZnO nanoparticle	MRSA	160 µg/mL	26
13.	amoxicillin, azithromycin and clarithromycin (antibiotic)	MRSA	>64 µg/mL	27
14.	Aminocellulose conjugate and hyaluronic acid on polymer nanoparticles	*S. aureus*	80 µg/mL	28
15.	CuO nanoparticles	*S. aureus*	>10 mg/mL	29
16.	Ampicillin and Cefotaxime (antibiotic)	*S. aureus*	>0.256 and 0.0015 mg/mL respectively	29
17.	Auranofin (gold salt)	MRSA	0.5 mg/L	30
18.	Al_2O_3 nanoparticles	MRSA	1,700 to 3,400 µg/mL	31
19.	Reduced graphene oxide-metal oxide (rGO-NiO/AgO/ZnO) nanocomposites	*S. aureus*	125, 250 and 125 µg/mL respectively	32
20.	CuO, NiO and CuO-NiO	*S. aureus*	4.5, 8.5 and 3 mg/mL respectively	33
21.	ZnO nanostructures	*S. aureus*	25 mg/L	34
22.	Antimicrobial peptides mimetic copolymers	*S. aureus*	125–250 µg/mL for butyl containing copolymers	35
23.	NP108 (antimicrobial polymer)	*S. aureus*	8 to 500 mg/L	36
24.	Cationic methacrylate polymers	*S. aureus*	~42-125 µg/mL	37
25.	ZnO nanoparticles	*S. aureus*	125 µg/mL	38
26.	Propolis and gentamycin based hydrogel	MRSA	41.6-83.3 µg/mL	39
27.	Alginate/ PVA silver nanocomposite hydrogel	*S. aureus*	250 µg/mL	40
28.	Levofloxacin-loaded hyaluronic acid nanohydrogel	*S. aureus*	0.104 ± 0.058 mg/L	41
29.	Vancomycin loaded pluronic–a-cyclodextrin supramolecular gel	*S. aureus*	1–4 mg/L	42
30.	Polycationic hydrogel	*S. aureus*	8-6300 µg/mL	43
31.	Chitosan/poly[(acrylic acid)-*co*-(2-hydroxyethyl methacrylate)] based nanocomposite hydrogels	*S. aureus*	1.56 mg/mL	44
32.	Peptide based supramolecular hydrogel	*S. aureus*	50-100 µg/mL	45
33.	trishexylaminomelamine Trisphenylguanide	*S. aureus*	1 mg/L	46
34.	AgNPs composing alginate/gelatine hydrogel	*S. aureus*	53.0 µg/mL	47
35.	Drug loaded peptide amphiphiles with heparin-binding cardin-motifs	MRSA	300 µg/ml	48
36.	Ag–ZnO nanocomposite	*S. aureus*	60 µg/mL	49

37.	PVA AgNPs	*S. aureus*	≥54 µg/mL	50
38.	Silver doped ZnO nanoparticles	*S. aureus*	4-10 mg/mL	51
39.	Ag nanoclusters encapsulated in silica nanospheres	*S. aureus*	0.3 mg/mL	52
40.	Meropenem and cefixime metal ion (Cd, Ag, Pd, Ni, Zn, Cu) complexes	*S. aureus*	50-500 µg/mL	53
41.	Multiwalled carbon nanotube/ZnO nanoparticles hybrid material	*S. aureus*	0.25 mg/mL	54
42.	MgO Nanoparticles	*S. aureus*	0.075 mg/mL	55
43.	AgNPs confined in silica-based calcium phosphate	*S. aureus*	20 mg/mL	56

References

1. Singh A, Nisaa K, Bhattacharyya S, Mallick AI. Immunogenicity and protective efficacy of mucosal delivery of recombinant hcp of Campylobacter jejuni Type VI secretion system (T6SS) in chickens. Mol. Immunol. 2019;111:182-97.
2. Anh HTP, Huang CM, Huang CJ. Intelligent metal-phenolic metallogels as dressings for infected wounds. Sci. Rep. 2019;9:11562.
3. Mitra S, Kandambeth S, Biswal BP, Khayum MA, Choudhury CK, Mehta M, Kaur G, Banerjee S, Prabhune A, Verma S, Roy S. Self-exfoliated guanidinium-based ionic covalent organic nanosheets (iCONs). J. Am. Chem. Soc. 2016;138:2823–8.
4. Ghosh R, Malhotra M, Sathe RRM, Jayakannan M. Biodegradable polymer theranostic fluorescent nanoprobe for direct visualization and quantitative determination of antimicrobial activity. Biomacromolecules. 2020;21:2896–912.
5. Quinteros MA, Aristizábal VC, Dalmasso PR, Paraje MG, Páez PL. Oxidative stress generation of silver nanoparticles in three bacterial genera and its relationship with the antimicrobial activity. Toxicol. in vitro. 2016;36:216–23.
6. Singh A, Nisaa K, Bhattacharyya S, Mallick AI. Immunogenicity and protective efficacy of mucosal delivery of recombinant hcp of Campylobacter jejuni Type VI secretion system (T6SS) in chickens. Mol. Immunol. 2019;111:182–97.
7. Dholvitayakhun A, Cushnie TPT, Trachoo N. Antibacterial activity of three medicinal Thai plants against Campylobacter jejuni and other foodborne pathogens. Nat. Prod. Res. 2012;26:356–63.
8. Campana R, Patrone V, Franzini ITM, Diamantini G, Vittoria E, Baffone W. Antimicrobial activity of two propolis samples against human Campylobacter jejuni. J. Med. Food. 2009;12:1050–6.
9. Lu X, Samuelson DR, Rasco BA, Konkel ME. Antimicrobial effect of diallyl sulphide on Campylobacter jejuni biofilms. J. Antimicrob. Chemother. 2012;67:1915–26.

10. Gahamanyi N, Song DG, Cha KH, Yoon KY, Mboera LEG, Matee MI, Mutangana D, Amachawadi RG, Komba EVG, Pan CH. Susceptibility of Campylobacter strains to selected natural products and frontline antibiotics. Antibiotics. 2020;9:790.
11. Oh E, Jeon B. Contribution of surface polysaccharides to the resistance of Campylobacter jejuni to antimicrobial phenolic compounds. J. Antibiot. 2015;68:591–3.
12. Rossi PG, Bao L, Luciani A, Panighi J, Desjobert JM, Costa J, Casanova J, Bolla JM, Berti L. (E)-Methylisoeugenol and elemicin: antibacterial components of Daucus carota L. essential oil against Campylobacter jejuni. J. Agric. Food Chem. 2007;55:7332–6.
13. Klančnik A, Možina SS, Zhang Q. Anti-Campylobacter activities and resistance mechanisms of natural phenolic compounds in Campylobacter. PloS one. 2012;7:e51800.
14. Dufour V, Alazzam B, Ermel G, Thepaut M, Rossero A, Tresse O, Baysse C. Antimicrobial activities of isothiocyanates against Campylobacter jejuni isolates. Front. Cell. Infect. Microbiol. 2012;2:53.
15. Ribeiro LNM, de Paula E, Rossi DA, Martins FA, de Melo RT, Monteiro GP, Breikreitz MC, Goilart LR, Fonseca BB. Nanocarriers From Natural Lipids With In Vitro Activity Against Campylobacter jejuni. Front. Cell. Infect. Microbiol. 2021;10:571040.
16. He Y, Ingudam S, Reed S, Gehring A, Strobaugh Jr TP, Irwin P. Study on the mechanism of antibacterial action of magnesium oxide nanoparticles against foodborne pathogens. J. Nanobiotechnol. 2016;14:54.
17. Mun SH, Joung DK, Kim YS, Kang OH, Kim SB, Seo YS, Kim YC, Lee DS, Shin DW, Kweon KT, Kwon DY. Synergistic antibacterial effect of curcumin against methicillin-resistant Staphylococcus aureus. Phytomedicine. 2013;20:714–8.
18. Akiyama H, Fujii K, Yamasaki O, Iwatsuki K. Antibacterial action of several tannins against Staphylococcus aureus. J. Antimicrob. Chemother. 2001;48:487–91.
19. Tsuchiya H, Sato M, Miyazaki T, Fujiwara S, Tanigaki S, Ohyama M, Tanaka T, Iinuma M. Comparative study on the antibacterial activity of phytochemical flavanones against methicillin-resistant Staphylococcus aureus. J. Ethnopharmacol. 1996;50:27–34.
20. Bolatchiev A. Antibacterial activity of human defensins against Staphylococcus aureus and Escherichia coli. PeerJ, 2020;8:e10455.
21. Kim SH, Lee HS, Ryu DS, Choi SJ, Lee DS. Antibacterial activity of silver-nanoparticles against Staphylococcus aureus and Escherichia coli. Korean J. Microbiol. Biotechnol. 2011;39:77–85.
22. Xie N, Jiang L, Chen M, Zhang G, Liu Y, Li J, Huang X. In vitro and in vivo antibacterial activity of linezolid plus fosfomycin against Staphylococcus aureus with resistance to one drug. Infect. Drug Resist. 2021;14:639.
23. Dong G, Liu H, Yu X, Zhang X, Lu H, Zhou T, Cao J. Antimicrobial and anti-biofilm activity of tannic acid against Staphylococcus aureus. Nat. Prod. Res. 2018;32:2225–8.

24. Sheikholeslami S, Mousavi SE, Ashtiani HRA, Doust SRH, Rezayat SM. Antibacterial activity of silver nanoparticles and their combination with zataria multiflora essential oil and methanol extract. Jundishapur J. Microbiol. 2016;9:e36070.
25. Punjabi K, Mehta S, Chavan R, Chitalia V, Deogharkar D, Deshpande S. Efficiency of biosynthesized silver and zinc nanoparticles against multi-drug resistant pathogens. Front. Microbiol. 2018;9:2207.
26. Kadiyala U, Turali-Emre ES, Bahng JH, Kotov NA, Scott VanEpps J. Unexpected insights into antibacterial activity of zinc oxide nanoparticles against methicillin resistant Staphylococcus aureus (MRSA). Nanoscale. 2018;10:4927–39.
27. Akram FE, El-Tayeb T, Abou-Aisha K, El-Azizi M. A combination of silver nanoparticles and visible blue light enhances the antibacterial efficacy of ineffective antibiotics against methicillin-resistant Staphylococcus aureus (MRSA). Ann. Clin. Microbiol. Antimicrob. 2016;15:48.
28. Ivanova A, Ivanova K, Hoyo J, Heinze T, Sanchez-Gomez S, Tzanov T. Layer-By-Layer Decorated Nanoparticles with Tunable Antibacterial and Antibiofilm Properties against Both Gram-Positive and Gram-Negative Bacteria. ACS Applied Mater. Interfaces. 2018;10:3314–23.
29. Khan S, Ansari AA, Khan AA, Abdulla M, Al-Obaid O, Ahmad R. In vitro evaluation of cytotoxicity, possible alteration of apoptotic regulatory proteins, and antibacterial activity of synthesized copper oxide nanoparticles. Colloids Surf. B. 2017;153:320–6.
30. Harbut MB, Vilcheze C, Luo X, Hensler ME, Guo H, Yang B, Chatterjee AB, Nizet V, Jacobs Jr WR, Schultz PG, Wang F. Auranofin exerts broad-spectrum bactericidal activities by targeting thiol-redox homeostasis. Proc. Nat. Acad. Sci. 2015;112:4453–8.
31. Ansari MA, Khan HM, Kha AA, Pal R, Cameotra SS. Antibacterial potential of Al_2O_3 nanoparticles against multidrug resistance strains of Staphylococcus aureus isolated from skin exudates. J. Nanoparticle Res. 2013;15:1970.
32. Elbasuney S, El-Sayyad GS, Tantawy H, Hashem AH. Promising antimicrobial and antibiofilm activities of reduced graphene oxide-metal oxide (RGO-NiO, RGO-AgO, and RGO-ZnO) nanocomposites. RSC Adv. 2021;11:25961–75.
33. Paul D, Neogi S. Synthesis, characterization and a comparative antibacterial study of CuO, NiO and CuO-NiO mixed metal oxide. Mater. Res. Express. 2019;6:055004.
34. Kumar KM, Mandal BK, Naida EA, Sinha M, Kumar KS, Reddy PS. Synthesis and characterisation of flower shaped Zinc Oxide nanostructures and its antimicrobial activity. Spectrochim. Acta A. 2013;104:171–4.
35. Sovadinova I, Kuroda K, Palermo EF. Unexpected enhancement of antimicrobial polymer activity against Staphylococcus aureus in the presence of fetal bovine serum. Molecules. 2021;26:4512.

36. Mercer DK, Katvars LK, Hewitt F, Smith DW, Robertson J, O'Neill DA. NP108, an Antimicrobial Polymer with Activity against Methicillin- and Mupirocin-Resistant Staphylococcus aureus. Antimicrob. Agents Chemother. 2017;61:e00502-17.
37. Thoma LM, Boles BR, Kuroda K. Cationic Methacrylate Polymers as Topical Antimicrobial Agents against Staphylococcus aureus Nasal Colonization. Biomacromolecules. 2014;15:2933–43.
38. Siddiqi KS, ur Rahman A, Tajuddin, Husen A. Properties of Zinc Oxide Nanoparticles and Their Activity Against Microbes. Nanoscale Res. Lett. 2018;13:141.
39. Gezgin Y, Kazan A, Ulucan F, Yesil-Celiktas O. Antimicrobial activity of propolis and gentamycin against methicillinresistant Staphylococcus aureus in a 3D thermo-sensitive hydrogel. Ind. Crops Prod. 2019;139:111588.
40. Ghasemzadeh H, Ghanaat F. Antimicrobial alginate/PVA silver nanocomposite hydrogel, synthesis and characterization. J. Polym. Res. 2014;21:355.
41. Montanari E, D'Arrigo G, Meo CD, Virga C, Coviello T, Passariello C, Matricardi P. Chasing bacteria within the cells using levofloxacin-loaded hyaluronic acid nanohydrogels. Eur. J. Pharm. Biopharm. 2014;87:518–23.
42. Simoes SMN, Veiga F, Torres-Labandeira JJ, Ribeiro ACF, Sandez-Macho MI, Concheiro A, Alvarez-Lorenzo C. Syringeable Pluronic–α-cyclodextrin supramolecular gels for sustained delivery of vancomycin. Eur. J. Pharm. Biopharm. 2012;80:103–12.
43. Li P, Poon YF, Li W, Zhu HY, Yeap SH, Cao Y, Qi X, Zhou C, Lamrani M, Beuerman RW, Kang ET, Mu Y, Li CM, Chang MW, Leong, SSJ, Chan-Park MB. A polycationic antimicrobial and biocompatible hydrogel with microbe membrane suctioning ability. Nat. Mater. 2010;10:149–56.
44. Noppakundilograt S, Sonjaipanich K, Thongchul N, Kiatkamjornwong S. Syntheses, characterization, and antibacterial activity of chitosan grafted hydrogels and associated mica-containing nanocomposite hydrogels. J. Appl. Polym. Sci. 2013;127:4927–38.
45. Nandi N, Gayen K, Ghosh S, Bhunia D, Kirkham S, Sen SK, Ghosh S, Hamley IW, Banerjee A. Amphiphilic Peptide-based Supramolecular, Non-Cytotoxic Stimuli-responsive Hydrogels with Antibacterial Activity. Biomacromolecules. 2017;18:3621–29.
46. Weaver Jr AJ, Shepard JB, Wilkinson RA, Watkins RL, Walton SK, Radke AR, Wright TJ, Awel MB, Cooper C, Erikson E, Labib ME, Voyich JM, Teintze M. Antibacterial Activity of THAM Trisphenylguanide against Methicillin-Resistant Staphylococcus aureus. PloS one. 2014;9:e97742.
47. Diniz FR, Maia RCAP, de Andrade LRM, Andrade LN, Chaud MV, da Silva CF, Correa CB, de Albuquweque RL, da Costa LP, Shin SR, Hassan S, Sanchez-Lopez E, Souto EB, Severino P. Silver Nanoparticles-Composing Alginate/Gelatine Hydrogel Improves Wound Healing In Vivo. Nanomaterials. 2020;10:390.

48. Chang R, Subramanian K, Wang M, Webster TJ. Enhanced Antibacterial Properties of Self-Assembling Peptide Amphiphiles Functionalized with Heparin-Binding Cardin-Motifs. ACS Appl. Mater. Interfaces. 2017;9:22350–60.
49. Matai I, Sachdev A, Dubey P, Kumar SU, Bhushan B, Gopinath P. Antibacterial activity and mechanism of Ag–ZnO nanocomposite on S. aureus and GFP-expressing antibiotic resistant E. coli. Colloids Surf. B. 2014;115:359–67.
50. Cavassin ED, de Figueiredo LFP, Otoch JP, Seckler MM, de Oliveira RA, France FF, Marangoni VS, Zucolotto V, Levin ASS, Costa SF. Comparison of methods to detect the in vitro activity of silver nanoparticles (AgNP) against multidrug resistant bacteria. J. Nanobiotechnol. 2015;13:64.
51. Sharma N, Kumar J, Thakur S, Sharma S, Shrivastava V. Antibacterial study of silver doped zinc oxide nanoparticles against Staphylococcus aureus and Bacillus subtilis. Drug Invent. Today. 2013;5:50–4.
52. Lu R, Zou W, Du H, Wang J, Zhang S. Antimicrobial activity of Ag nanoclusters encapsulated in porous silica nanospheres. Ceram. Int. 2014;40:3693–8.
53. Umekar MJ, Lohiya RT, Gupta KR, Kotagale NR, Raut NS. Studies on meropenem and cefixime metal ion complexes for antibacterial activity. Future J. Pharm. Sci. 2021;7:233.
54. Rafique S, Bashir S, Akram R, Kiyani FB, Raza S, Hussain M, Fatima SK. Variation in the Performance of MWCNT/ZnO Hybrid Material with pH for Efficient Antibacterial Agent. BioMed Res. Int. 2022;1300157.
55. Baniasadi N, Kariminik A, Khoshroo SMR. Synthesis of MgO Nanoparticles and Their Antibacterial Properties on Three Food Poisoning Causing Bacteria. Iran. J. Med. Microbiol. 2019;13:380–91.
56. Kung JC, Wang WH, Lee CL, Hsieh HC, Shih CJ. Antibacterial Activity of Silver Nanoparticles (AgNP) Confined to Mesostructured, Silica-Based Calcium Phosphate against Methicillin-Resistant Staphylococcus aureus (MRSA). Nanomaterials. 2020;10:1264.